Experimental demonstration of an end-burning swirling flow hybrid rocket engine

Jean-Yves Lestrade, Jérôme Anthoine, Anthony J. Musker, Anthony Lecossais

▶ **To cite this version:**

Jean-Yves Lestrade, Jérôme Anthoine, Anthony J. Musker, Anthony Lecossais. Experimental demonstration of an end-burning swirling flow hybrid rocket engine. Aerospace Science and Technology, 2019, 92, pp.1-8. 10.1016/j.ast.2019.05.057 . hal-02299059

HAL Id: hal-02299059
https://hal.science/hal-02299059

Submitted on 6 Nov 2019

HAL is a multi-disciplinary open access archive for the deposit and dissemination of scientific research documents, whether they are published or not. The documents may come from teaching and research institutions in France or abroad, or from public or private research centers.

L'archive ouverte pluridisciplinaire **HAL**, est destinée au dépôt et à la diffusion de documents scientifiques de niveau recherche, publiés ou non, émanant des établissements d'enseignement et de recherche français ou étrangers, des laboratoires publics ou privés.

Experimental Demonstration of an End-Burning Swirling Flow Hybrid Rocket Engine

J-Y. Lestrade[a,*], J. Anthoine[a], A. J. Musker[b], A. Lecossais[c]

[a] *ONERA - The French Aerospace Lab, F-31410, Mauzac, France*
[b] *DELTACAT Ltd, Kintyre House, 70 High Street, Fareham, Hampshire, PO16 7BB, UK, and Visiting Professor, Aeronautics and Astronautics Unit, University of Southampton, UK*
[c] *Airbus Defence and Space, F-31400 Toulouse, France*

Abstract

Within the framework of the European H2020 HYPROGEO program, an innovative hybrid engine combustion chamber compatible with satellite requirements (constant thrust over very long burn-times) had to be developed. A first test rig was designed and tested in order to better understand the functioning of this innovative combustion chamber, and to help the design of a breadboard to demonstrate the efficiency of this new engine with respect to the mission requirements. Two test campaigns, the first on the test rig with 87.5% hydrogen peroxide, and the second on the hybrid engine breadboard with 98% hydrogen peroxide, were performed under various operating conditions to demonstrate the catalytic ignitability of this new hybrid engine, and the sustainment of a stable combustion over firing durations up to 180 s. The test campaigns also enabled the identification of the main influencing parameter on the fuel regression rate for this innovative combustion chamber.

Keywords: Hybrid propulsion; H2020 HYPROGEO project; Innovative combustion chamber; Experimental demonstration; End-burning swirling-flow

*Corresponding author
Email address: jean-yves.lestrade@onera.fr (J-Y. Lestrade)

1. Introduction

The use of electrical propulsion systems to transfer satellites from GTO to operational GEO orbits, in addition to their current use for station-keeping, seems to be the trend for future European telecommunication satellites. However, the long transfer durations inherent to such low-thrust technologies may not be compatible with all mission timeline requirements. One of the solutions proposed by industry and public agencies is to employ a dedicated high-thrust propulsion system to accelerate the transfer phase. This apogee kick-stage module should also combine environmentally-friendly chemical technology and electrical thrusters, to optimize its efficiency in terms of propulsive performances, mass, costs, etc.

Owing to their advantages over current MMH/NTO bi-propellant engines, such as increased safety, lower environmental impact, better propulsive performances, lower costs, etc., hybrid propulsion systems could be a good candidate for this task. However, the current architecture of such an engine is not suitable for the long burn-time and constant-thrust required for a satellite application, as a result of the variations in oxidizer-to-fuel ratio and fuel grain shape with time. An innovative combustion chamber satisfying the previous requirements is thus to be developed.

In order to have a constant thrust, Rice *et al.* developed the vortex end-burning hybrid engine (VEBH) which provides the advantage of a constant fuel burning surface area [1]. The engine mixture ratio can be controlled by varying the oxidizer mass flow rate and/or the combustion chamber diameter (fuel surface area). As presented in Figure 1, this engine, designed for use with HTPB, consists of a ring chamber sandwiched between top and bottom matings, with the gaseous oxidizer (GOX) tangentially injected through ports at the tail-end (nozzle side) of the chamber in order to create a swirl motion of the gaseous phase, and to increase the fuel regression rate. Based on observations of post-firing fuel grains, a counter-swirling pattern of grooves, which appear to indicate flow opposite to that of the swirl GOX injection, exists near the centre of the

chamber. According to the authors, a portion of the oxygen may be spiralling along the bottom of the chamber and up to the head end in the central region, where it meets the grain surface and flows back outward. In this case, the flow field might consist of two inter-twined spirals in the central region of the chamber, one spinning upward and the other spinning downward towards the nozzle (Figure 2). However, this concept is not compatible with the long burn-

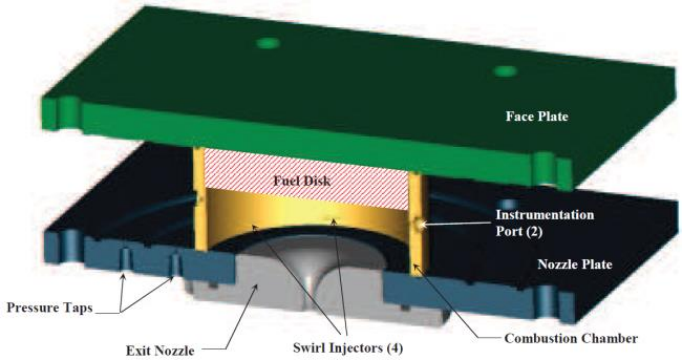

Figure 1: Vortex end-burning hybrid engine [1]

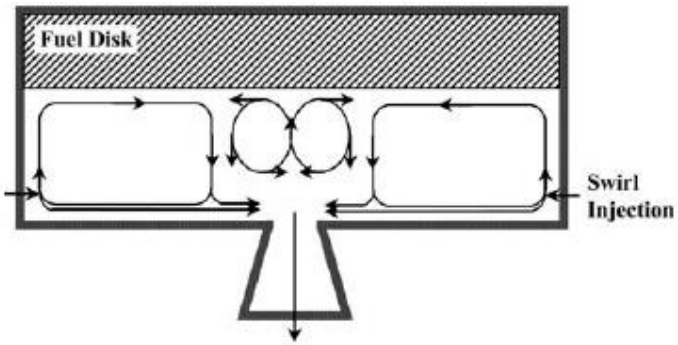

Figure 2: Flow field in the combustion chamber [2]

time required for satellite applications, since the distance between the injection location and the fuel surface evolves with time, which may cause combustion stability and ignition issues. In order to solve this problem, an interesting solution is the end-burning swirling-flow hybrid rocket engine (named SOFT for Swirling Oxidizer Flow Type), using paraffin wax developed by Hayashi and Sakurai for

application to a first stage [3]. This concept is similar to that of Rice et al. in terms of overall dimensions, oxidizer type and injection, but is equipped with an actuator to push the fuel grain axially toward the nozzle side in order to keep the volume of the combustion chamber constant during burning. As in the previous study, the authors observed that the fuel regressed axially with a high regression rate region close to the centre of the fuel grain. According to Volchkov *et al.*, the convection coefficient on the surface is maximum at the axis level because of the phenomena induced by the swirl injection [4]. Hayashi and Sakurai concluded that the formation of a crater at the centre of the fuel grain was provoked by these same mechanisms, since the energy input was higher.

Although this concept was interesting, the actuator was not useful, as a result of the very short burn duration (only two seconds). Moreover, the fuel employed for this study was not suitable for use on-board a satellite due to its high regression rate: the length needed to make this engine compatible with the requirements in terms of burn duration would make it incompatible with spacecraft sizing. Dedicated studies on pancake hybrid engines were performed in order to satisfy these constraints [5, 6], but these concepts led to a time-variant change in the oxidizer-to-fuel ratio and the fuel grain shape, which is not coherent with the satellite requirements for constant thrust.

Within the framework of the European H2020 HYPROGEO project, a hybrid engine compatible with a long burn duration (about 5000 s) and with a constant thrust at the required level (250 N) for use on-board a spacecraft had to be developed [7]. To reach these objectives, the idea was to design an end-burning, swirling-flow hybrid engine combined with a passive actuator to compensate for the fuel regression, operating with high density polyethylene as fuel and 98% hydrogen peroxide as oxidizer; this type of fuel is suitable for use on-board satellites due to its very low regression rate. In addition, catalytic injection combining start and stop capabilities is made possible by the choice of this oxidizer.

The methodology that was followed during the HYPROGEO project led to the development of two innovative hybrid rocket engines. The first one, the

MHYCAS facility [8], was designed to better understand the functioning of this new combustion chamber architecture, while the goal of the second one, the SuperMHYCAS facility, was to demonstrate the efficiency of this new engine with respect to the objectives for constant thrust over long burn durations. This paper will consequently describe the architecture of these new hybrid engines and discuss the test results.

2. The MHYCAS test campaign

The MHYCAS engine (Figure 3), a French acronym for 'hybrid engine compatible with satellite application', was designed and tested as an intermediate step in order to better define the final breadboard of the HYPROGEO project, to investigate potential difficulties, such as catalytic ignition or oxidizer injection, and to define the operating conditions to have the required oxidizer-to-fuel ratio, chamber pressure and oxidizer mass flow rate.

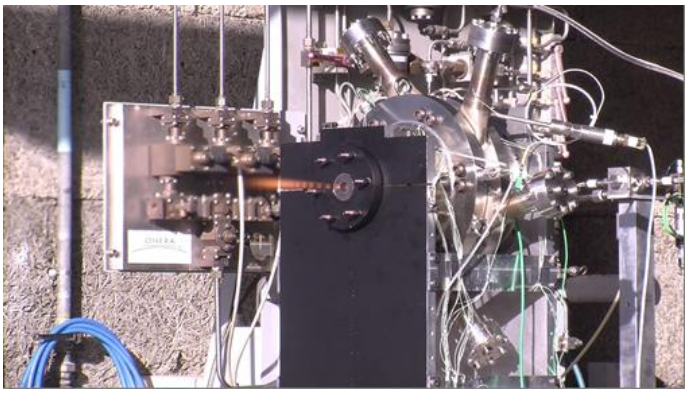

Figure 3: MHYCAS hybrid engine during a test firing

2.1. Description of the test facility

The MHYCAS facility is composed of a pressurized tank, feeding lines, and the MHYCAS hybrid engine. The tank pressure is maintained at a constant level during the firing test to keep the oxidizer mass flow rate, and hence operating conditions, constant.

The MHYCAS engine (Figure 4) is composed of a fuel tank containing the high density polyethylene fuel grain, an annular ring providing a swirl injection, with six decomposition chambers filled with the platinum-based PX1 catalyser and supplied with 87.5% hydrogen peroxide mounted to the annular ring (Figure 5), a combustion chamber of 200 mm in-diameter at the fuel location, and a nozzle with an adaptable throat section. The modular design of this hybrid engine enables the operator to easily change the number of active decomposition chambers, the initial position of the fuel grain with respect to the location of the oxidizer slots, the shape of the fuel grain, and the operating conditions in terms of chamber pressure, oxidizer mass flow rate and mass flux (calculated at oxidizer injection). However, contrary to the VEHB and SOFT engines, the oxidizer injection is located very close to the fuel grain to ease the catalytic ignition of the engine. Moreover, since the oxidizer injection and the gaseous flow have a major impact on the fuel regression rate, the ring was designed with the help of idealised and CFD analyses [9]. These analyses led to the selection of six continuous ducts which inject the oxidizer tangentially to the combustion chamber to generate a swirling motion (Figure 5). The engine is equipped with temperature and pressure probes located at the end of one of the six decomposition chambers, and three pressure probes placed around the combustion chamber. The engine is also placed on a thrust bench to measure the propulsive performance. However, it should be noted that the nozzle was not adapted to ambient pressure, since the nozzle throat was only modified to target different values of combustion chamber pressure.

To complete these measurements, thin thermocouples were welded onto the external wall of the engine: 14 were placed on the combustion chamber, one was placed at the end of each decomposition chamber, and two were placed on the fuel tank. By means of a backwards integration method, these temperature measurements enable the evaluation of the inside wall temperature and the thermal flux along the combustion chamber.

Finally, the instrumentation for the test facility includes a Coriolis mass flow meter and temperature and pressure transducers for the liquid oxidizer,

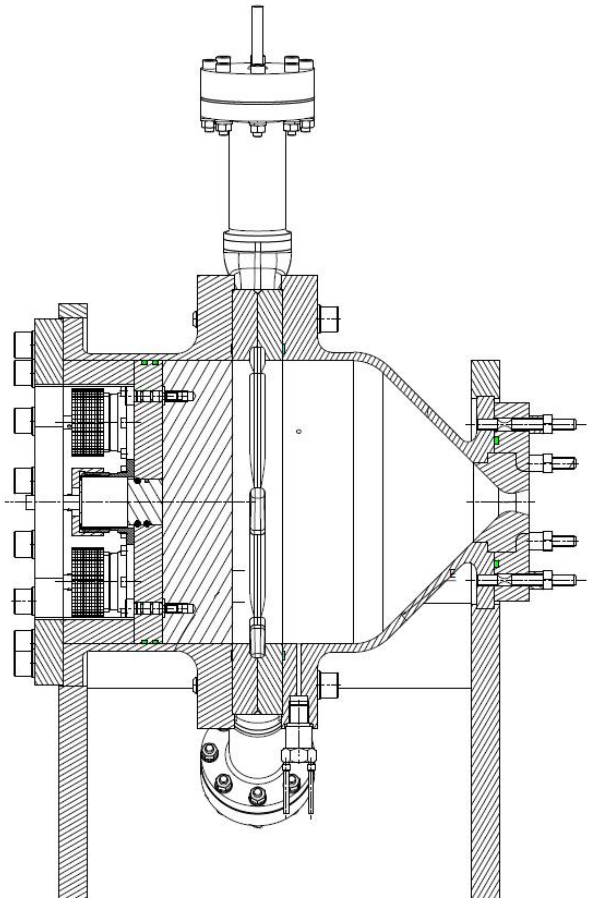

Figure 4: Drawing of the MHYCAS engine

upstream of the oxidizer distributor. The latter distributes the oxidizer from the main supply line to the six secondary lines, each one being connected to a single decomposition chamber.

The uncertainties related to the measurement techniques implemented on this test bench are specified in Table 1.

2.2. Test results

The MHYCAS test campaign was performed through 25 test firings with the same test sequence. As presented in Figure 6, the first phase of the firing tests corresponded to a blipping sequence of the oxidizer injection, to fill the oxidizer

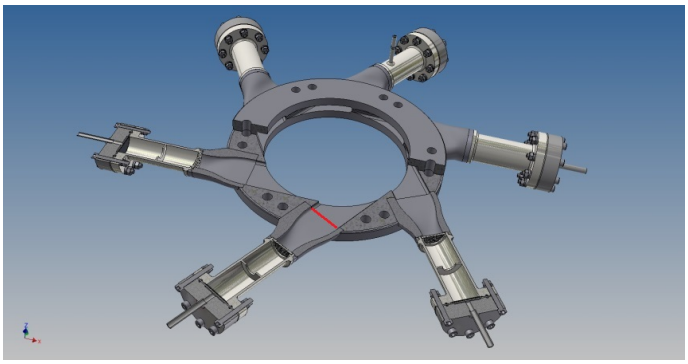

Figure 5: Drawing of the selected injector ring with the decomposition chambers

Table 1: Uncertainties of the measurements techniques implemented on the MHYCAS facility

Quantity	**Uncertainty**	**Unit**
Pressure	1000	Pa
Oxidizer mass flow rate	0.1	g/s
Temperature	1	k
Thrust	2	N

lines and to slowly warm-up the decomposition chambers to avoid damaging the catalyser. This sequence was followed by a continuous oxidizer injection phase, which can be split into two parts: a mono-propellant phase, where the combustion process has not started, and a hybrid phase as soon as the engine has ignited. Finally, after the firing test, a drain phase was employed, which consisted of a continuous nitrogen injection to avoid thermal lag and degradation of the engine. This phase was also composed of two distinct parts: the first was the flushing of the hydrogen peroxide contained in the feed lines (associated with an increase in chamber pressure during the flush), whilst the second was the injection of pure nitrogen into the engine. The objectives of the first four tests were to ignite the hybrid engine, and to maintain a stable hybrid mode over several seconds. These tests revealed that the engine was able to ignite, but also that the fuel grain position with respect to the oxidizer injection location had a

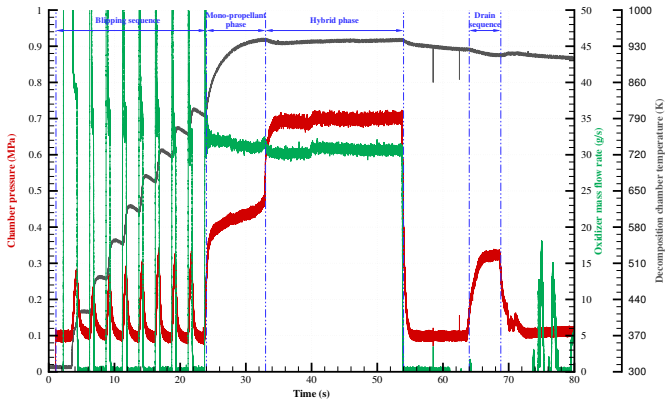

Figure 6: Example of the firing test phases for the MHYCAS engine

major influence on the ignition delay. This distance was set to 12.5 mm for the first two firing tests, and was then fixed at 1 mm for the rest of the test campaign, in order to minimize the monopropellant phase duration. Several configurations were then tested through the campaign at various operating conditions, in terms of pressure or mass flow rate. In order to increase the oxidizer mass flux at the injection, data evaluated in the cross section at the end of the injector duct r(ed line in Figure 5), two solutions were employed: the first consisted of reducing the number of active decomposition chambers (and consequently, the number of active decomposition injectors), and the second consisted of adding a circumferential plate around the fuel grain to reduce the oxidizer slot thiwkness and consequently the cross-sectional area of the active injectors. The results of the main tests are presented in Table 2. The oxidizer mass flux is evaluated at

It should be noted that to avoid the transient effects of the engine ignition, which could have a significant impact on the data for small-duration tests all the values provided were averaged over the last three seconds of hybrid phase duration. Moreover, the fuel regression rates values are only based on the fuel mass loss, and were corrected in the hybrid phase to consider the drain phase, where the engine re-ignited due to the hydrogen peroxide flush.

Table 2: MHYCAS firing test results

MHYCAS test number	**02**	**05**	**07**	**09**	**12**	**15**	**16**	**17**
Number of active decomposition chambers	6	6	6	3	3	6	2	2
Oxidizer slot thickness (mm)	10.5	10.5	10.5	10.5	10.5	10.5	10.5	3.5
Ignition delay (s)	19.2	35.0	3.7	6.6	4.2	8.6	7.5	9.2
Firing duration (s)	12.7	18.0	28.8	36.2	29.1	23.8	25.3	22.9
Chamber pressure (bar)	7.87	8.24	17.89	8.54	18.26	11.03	7.67	7.02
Oxidizer mass flow rate (g/s)	51.7	52.1	103.1	41.4	44.1	107.9	36.2	30.6
Oxidizer mass flux ($kg/m^2/s$)	16.4	16.5	37.7	26.3	28.0	34.3	34.4	87.5
Oxidizer-to-fuel mass ratio (-)	34.5	21.3	27.5	13.9	16.2	29.2	11.7	7.4
Regression rate (mm/s)	0.050	0.082	0.126	0.100	0.124	0.124	0.104	0.142
Experimental characteristic velocity (m/s)	1049	1071	1187	1364	1276	1212	1386	1436
Combustion efficiency (%)	89.2	82.9	96.8	96.0	93.0	100.0	93.7	89.9

The first firing tests were conducted with high oxidizer-to-fuel mass ratios compared with the target value of 7.4, which corresponds to the optimal value for a hybrid engine operating with 98% hydrogen peroxide and high-density polyethylene as propellants. Values very close to this target were reached with test MHYCAS_17 (two active decomposition chambers), and MHYCAS_22 (six active decomposition chambers), proving that reaching an optimum value of oxidizer-to-fuel ratio was feasible with such a hybrid engine.

2.3. Firing test analysis

The analysis of the firing tests presented in Table 2 will only focus on the behaviour of the fuel regression rate, since this parameter has a major role on the oxidizer-to-fuel ratio, and on the propulsive performances, which are two important criteria to optimize for applications to spacecraft.

The distance between the fuel grain surface and the oxidizer injection has a significant influence on the ignition delay. Consequently, it seems that the

heat transfer between the gaseous flow and the fuel grain is increased when this distance decreases. This is confirmed by comparing the MHYCAS_02 and MHYCAS_05 tests, for which the fuel regression rate has been significantly increased by reducing the distance between the fuel surface and the injector. This influence will not be present for the SuperMHYCAS engine, since the distance between the fuel surface and the oxidizer injection will remain constant by compensating for the fuel regression rate.

In a classical hybrid engine, pressure has no significant influence on the fuel regression rate. In order to verify if this assumption is correct with the MHYCAS engine, tests 07 and 15, as well as tests 09 and 12, can be compared in pairs, since they have similar oxidizer injection conditions with respect to mass flow rates and mass flux, but strong differences in combustion chamber pressures. It can be seen that the fuel regression rate is not modified when the pressure changes. This conclusion is verified whatever the value of the oxidizer mass flow rate, since it is true for high mass flow rates (geq 100 g/s), or low mass flow rates (leq 45 g/s). Note that these comparisons were performed on firing tests with the same number of active injectors. These results tend to show that the combustion chamber pressure has a negligible effect on the fuel regression rate.

The last factor which could have an important impact on the fuel regression rate is the oxidizer injection, which is well known for classical hybrid engine geometries. This can be separated further into various parameters, such as the mass flow rate, the mass flux, the injection velocity, and the injection geometry (the number of active decomposition chambers). When considering two firing tests with the same mass flow rates and mass fluxes, the only method of obtaining different oxidizer velocities is by changing the oxidizer density, which is achieved by modifying the chamber pressure. However, as discussed previously, the pressure, and thus the injection velocity of the oxidizer, does not have a significant influence on the regression rate. Based on a comparison of tests 16 and 17, and 15 and 22, it is possible to conclude that at a given number of active decomposition chambers and similar oxidizer mass flow rates, an increase in the mass flux improves the fuel regression rate. Finally, the number of active

decomposition chambers has a major impact on the fuel regression rate, since even with a similar oxidizer mass flow rate and a different oxidizer mass flux, tests 17 and 22 provided nearly identical oxidizer-to-fuel ratios. It seems that, for an oxidizer mass flux value, an increase in the number of active decomposition chambers increases the fuel regression rate.

3. The SuperMHYCAS test campaign

The objective of the SuperMHYCAS facility (Figure 7) was to demonstrate the efficiency of this innovative hybrid engine architecture with respect to the satellite requirements, namely providing a constant thrust over a long firing duration. In order to maximize the propulsive performances, this engine operates with 98% hydrogen peroxide, compared to the MHYCAS engine, which is only compatible with the standard grade of peroxide (87.5%). In order to sustain the high temperature expected during operation, most of the parts of the engine were manufactured in Inconel 625.

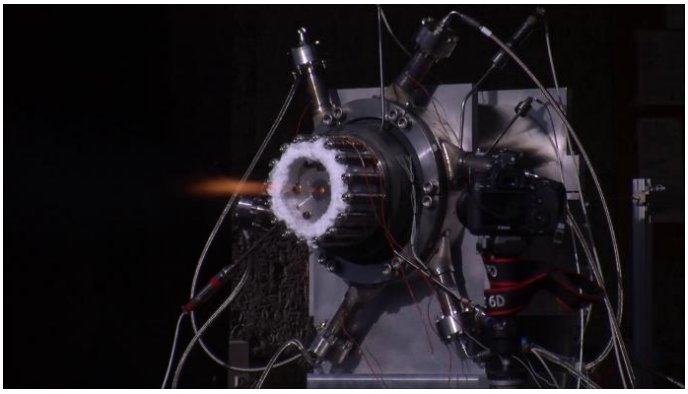

Figure 7: SuperMHYCAS hybrid engine

3.1. Description of the test facility

The design of the SuperMHYCAS engine (Figure 7) is very similar to the MHYCAS engine. The engine is composed of a fuel tank containing the high-

density polyethylene fuel grain, an annular ring providing a swirl injection, with six decomposition chambers filled with the PX1 catalyser mounted to the annular ring, a combustion chamber with a diameter of 250 mm at the location of the fuel grain, and a graphite nozzle with a throat diameter of 11.5 mm. This engine is thus slightly bigger than the MHYCAS engine, in order to be compatible with the thrust level required by the mission specifications. However, the design of the annular ring was performed in order to easily change the thickness of the oxidizer slot, since this parameter drives the oxidizer mass flux, which has a major impact on the fuel regression rate (main result of the MHYCAS test campaign). The injector ring (Figure 8) is composed of three parts, one external and two internal; the first internal part (in orange on Figure 9) sets the distance between the fuel grain and the oxidizer slot, while the other internal part (in blue on Figure 9) fixes the thickness of this slot.

The main difference with the design of the previous engine manufactured in the framework of this project lies in the addition of a passive fuel displacement system, in order to compensate for the fuel regression. The displacement of the fuel grain is guaranteed by the pressurisation, at a higher value than the combustion chamber pressure, of the volume located at the end the end-hand of the engine and the fuel grain is stoped at the opposite side (combustion chamber side) by the conical shape of annular injector ring.

The instrumentation of SuperMHYCAS facility is also very similar to that of the MHYCAS facility. The only difference lies in the addition of a linear displacement sensor to give an estimation of the fuel regression rate.

3.2. Test results and analysis

Eleven tests were performed during the SuperMHYCAS test campaign. The first four were dedicated to the adjustment of the test sequence, in order to avoid the extrusion of the fuel grain through the conical injection ring at the end of the firing test. The objective of the next three tests was to provide data through different oxidizer mass fluxes, in order to plot the evolution of the average fuel regression rate as a function of the oxidizer mass flux and of the oxidizer-to-fuel

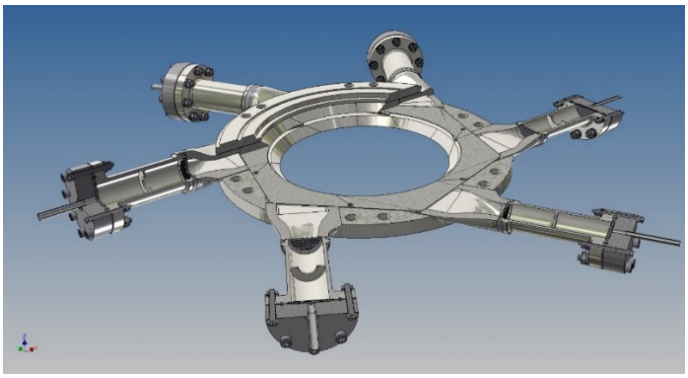

Figure 8: Complete assembly of the SuperMHYCAS injector ring

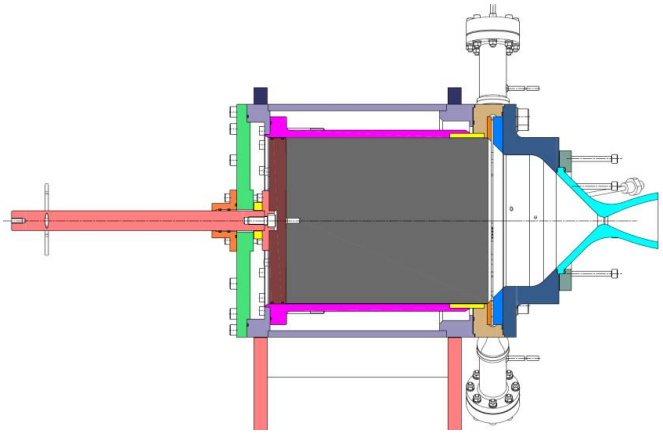

Figure 9: Drawing of the SuperMHYCAS engine

ratio. These two plots allow the determination of the thickness of the oxidizer injection slot needed to reach the optimum mixture ratio. The three tests were therefore performed under approximately the same operating conditions (Table 3) but with three different slot thicknesses (0.3, 0.6 and 2.8 mm). As with the MHYCAS test campaign, all the values provided were averaged over the last five seconds, to avoid significant effects of engine ignition and shut-off on the data averaging. The regression rate values are based on mass loss during the firing test.

Figure 10 presents the time evolutions of the chamber pressure, oxidizer

Table 3: SuperMHYCAS test results - tests 05 to 07

SuperMHYCAS test number	**05**	**06**	**07**
Slot thickness (mm)	0.6	2.8	0.3
Ignition delay (s)	9.7	7.2	22.5
Firing duration (s)	45.3	47.8	32.5
Chamber pressure (bar)	8.43	8.00	7.27
Oxidizer mass flow rate (g/s)	51.4	53.5	46.4
Decomposition temperature (K)	1176	1190	1188
Oxidizer-to-fuel mass ratio (-)	5.1	9.3	4.1
Regression rate (mm/s)	0.221	0.125	0.243

mass flow rate and decomposition chamber temperature observed during the sixth test of the SuperMHYCAS engine (with slot thickness of 2.8 mm). The evolutions for the two other tests were very similar. The blipping phase allowed for a gradual increase in decomposition chamber temperature before the continuous oxidizer injection, during which it reached about 1200 K. The monopropellant phase then started, and lasted until the engine was ignited and the hybrid phase began. Even if the oxidizer mass flow rate was constant during the hybrid mode, the chamber pressure evolved significantly, which meant that the transient phase for temperature was still not completed for this firing duration. The drop in the chamber pressure at the end of the firing test was due to the de-pressurization of the fuel grain tank, and the retraction of the fuel grain in order to avoid its extrusion into the combustion chamber when the oxidizer injection stopped. The data presented in Table 3 was collected in the five seconds before the depressurization of the fuel tank. Based on these three tests, the evolutions of the fuel regression rate as a function of the oxidizer-to-fuel ratio, and of the oxidizer mass flux, are plotted (Figure 11, Figure 12). Based on the interpolation equations of these two plots, an oxidizer-to-fuel ratio of 7.4 (the optimal value with respect to specific impulse for this configuration)

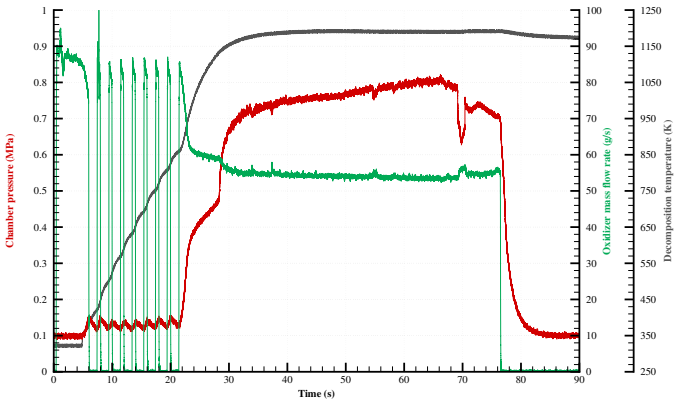

Figure 10: SuperMHYCAS_06 test results

corresponds to a fuel regression rate of 0.15 mm/s, and an oxidizer mass flux of 45.5 kg/m^2/s. Regarding the hybrid engine geometry, this last value leads to an oxidizer injection slot thickness of 1.65 mm. A new inner part of the injector ring, corresponding to this value, was subsequently manufactured and tested (SuperMHYCAS_08). The oxidizer-to-fuel ratio obtained during this test was 7.2 which was very close to the targeted value.

Later tests were performed to increase the firing duration up to 300 s, the maximum possible burn time based on transient thermoelastic computations at the optimal combustion efficiency for the combustion chamber. The SuperMHYCAS_09 and SuperMHYCAS_10 firing tests were performed under the same operating conditions over 90 and 180 s of continuous oxidizer injection, respectively. As presented in Figure 13, the data was very stable over the hybrid mode. The averaged results over the 5 s duration are listed in Table 4, and are comparable to the SuperMHYCAS_08 firing test results in terms of decomposition chamber temperature, chamber pressure, and oxidizer mass flow rate, even if the oxidizer mass flow rate for the final test is about 10% below the two previous tests, for an unexplained reason. However, the averaged oxidizer-to-fuel ratio continuously decreased as the firing duration increased. As presented in

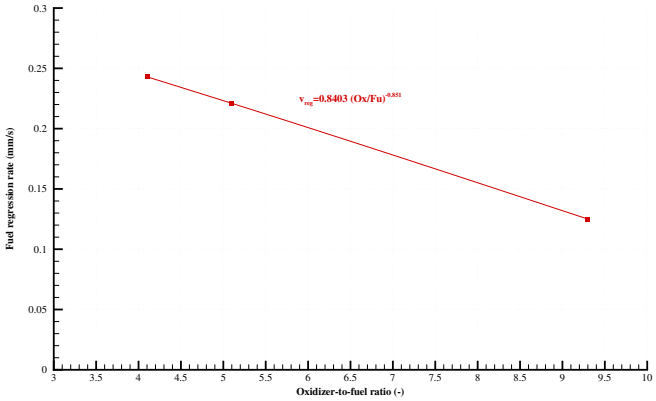

Figure 11: Evolution of the fuel regression rate as a function of the oxidizer to fuel ratio

Figure 14, the fuel grain displacement was non-linear, and increased with time. The reason for this evolution is still unexplained, but it justifies the decrease in the oxidizer-to-fuel ratio when the firing duration increases. Moreover, based on the observation of the fuel grain surfaces after the firing tests (Figure 15), the non-uniformity of the fuel regression rate over the burning surface has an influence on this evolution, but its quantification, if possible, is quite complex.

4. Conclusion

This paper presented the development of an innovative hybrid engine architecture compatible with satellite requirements (long burning duration associated with a constant thrust). To do this, two facilities were manufactured and tested.

The first, the MHYCAS facility, was designed to better understand the functioning of this new combustion chamber. The test campaign, performed with 87.5% hydrogen peroxide, was successful and achieved all the initial objectives. The catalytic ignitability of the fuel was demonstrated for various operating conditions: low and high oxidizer mass flow rates (from 30 to 110 g/s), low and medium combustion chamber pressures (from 5 to 20 bar), various numbers of active decomposition chambers, etc. The analysis revealed that the combustion

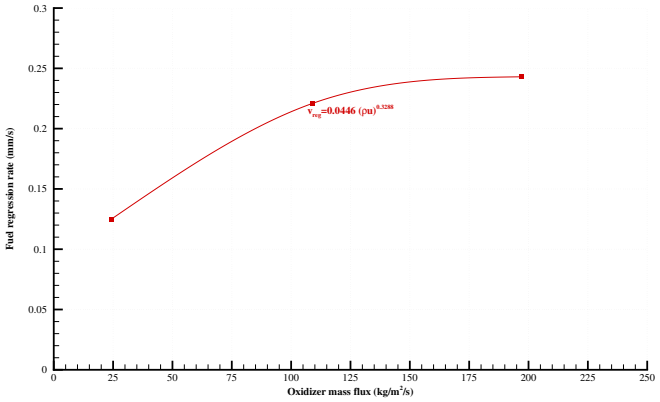

Figure 12: Evolution of the fuel regression rate as a function of the oxidizer mass flux

chamber pressure has no significant influence on the fuel regression rate, and that the main parameters influencing this regression rate are the number of active decomposition chambers, and the oxidizer mass flux.

The results of this first test campaign enabled the design of the SuperMHYCAS hybrid engine, with special attention being given to the oxidizer injection, in order to easily change its mass flux. The test campaign, performed with 98% hydrogen concentration, was also successful, with a combustion efficiency of about 90%. For a first engine of this size, and an engine that was not optimized with respect to thermal losses, this can be considered good. This test campaign included a 55 s firing test at the optimal average oxidizer-to-fuel ratio (7.4) for the required application, but as the firing duration increased, the averaged oxidizer-to-fuel ratio decreased, likely as a result of an escalation of the non-uniformity of the fuel regression rate over the burning surface. This should be addressed in further studies by working on the oxidizer injection..

Acknowledgements

This project received funding from the European Union's Horizon 2020 research and innovation programme, under grant agreement No 634534 entitled

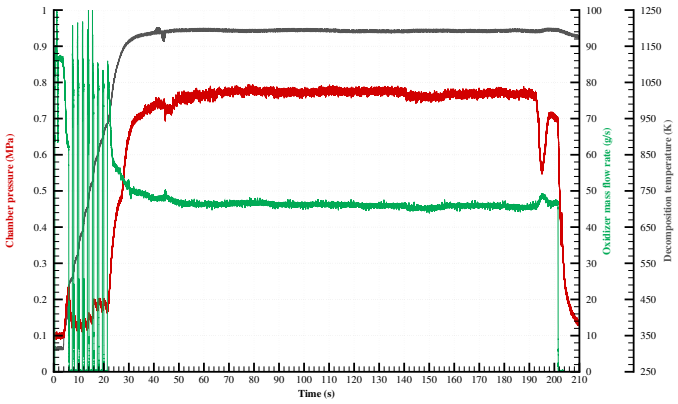

Figure 13: SuperMHYCAS_10 test results

"HYPROGEO Hybrid Propulsion Module for Transfer to GEO Orbit". The authors are grateful for this support.

References

[1] E. Rice, C. St. Clair, D. Gramer, M. J. Chiaverini, Mars ISRU CO/O2 rocket engine development and testing, in: 7th International Workshop on Microgravity Combustion and Chemically Reacting Systems, Cleveland, Ohio, 2003, hosted by NASA Glenn Research Center.

[2] M. J. Chiaverini, Review of Solid-Fuel Regression Rate Behavior in Classical and Nonclassical Hybrid Rocket Motors, in: Fundamentals of Hybrid Rocket Combustion and Propulsion, American Institute of Aeronautics and Astronautics, Reston ,VA, 2007, pp. 37–126. doi:10.2514/5.9781600866876.0037.0126.

[3] T. Sakurai, D. Hayashi, A Fundamental Study of a End-Burning Swirling-Flow Hybrid Rocket Engine using Low Melting Temperature Fuels, in: 51st AIAA/SAE/ASEE Joint Propulsion Conference, American Institute of Aeronautics and Astronautics, Reston, Virginia, 2015. doi:10.2514/6.2015-4138.

Table 4: SuperMHYCAS test results - tests 08 to 10

SuperMHYCAS test number	**08**	**09**	**10**
Slot thickness (mm)	1.65	1.65	1.65
Ignition delay (s)	7.1	5.5	5.9
Firing duration (s)	47.9	84.5	174.1
Chamber pressure (bar)	8.35	8.41	7.68
Oxidizer mass flow rate (g/s)	51.0	50.1	45.5
Oxidizer mass flux ($kg/m^2/s$)	109.1	24.3	196.9
Decomposition temperature (K)	1188	1198	1193
Oxidizer-to-fuel mass ratio (-)	7.2	6.0	5.0
Regression rate (mm/s)	0.154	0.182	0.198
Experimental characteristic velocity (m/s)	1493	1493	1462
Combustion efficiency (%)	91.5	90.4	89.2

[4] P. Volchkov, S. V. Semenov, V. I. Terekhov, Turbulent heat transfer at the forward face surface of a vortex chamber, Journal of Engineering Physics and Thermophysics 56 (2) (1989) 109.

[5] J. R. Caravella, S. D. Heister, E. J. Wernimont, Characterization of Fuel Regression in a Radial Flow Hybrid Rocket, Journal of Propulsion and Power 14 (1) (1998) 51–56. doi:10.2514/2.5265.

[6] G. S. Haag, M. N. Sweeting, G. Richardson, Low Cost Propulsion Development for Small Satellites at the Surrey Space Centre, in: 13th AIAA/USU Conference on Small Satellites, 1999, aIAA paper SSC99-XII-2.

[7] K. Odic, G. Denis, F. Ducerf, F. Martin, J.-Y. Lestrade, O. Verberne, J. Ryan, P. Christ, G. de Crombrugghe, HYPROGEO hybrid propulsion: project objectives & coordination, in: 6th International Symposium on Propulsion for Space Transportation, Space Propulsion, Rome, Italy, 2016.

[8] J.-Y. Lestrade, J. Messineo, J. Anthoine, A. Musker, F. Barato, Develop-

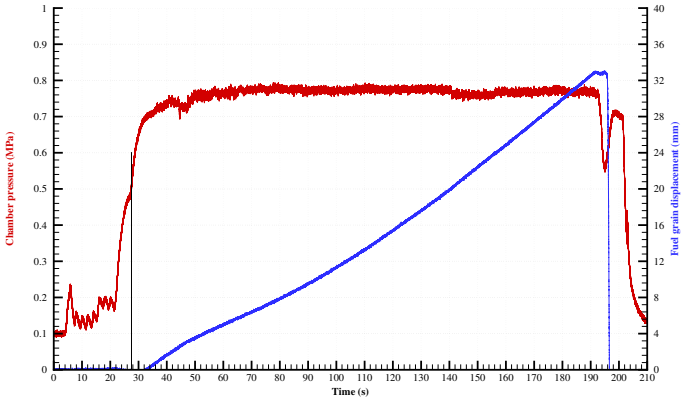

Figure 14: Evolution of the SuperMHYCAS_10 fuel grain displacement

ment and Test of an Innovative Hybrid Rocket Combustion Chamber, in: 7th European Conference for Aeronautics ans Space Sciences (EUCASS), Milan, Italy, 2017. doi:10.13009/EUCASS2017-414.

[9] A. Musker, J.-Y. Lestrade, J. Anthoine, A. Lecossais, Catalytic Injectors for an Isochoric Hybrid Rocket Motor, in: 7th International Symposium on Propulsion for Space Transportation, Space Propulsion, Seville, Spain, 2018.

Figure 15: Fuel grain surface after SuperMHYCAS_08 (top) and SuperMHYCAS_10 (bottom) firing tests